Automated Noncontact Facial Topography Mapping, 3-Dimensional Printing, and Silicone Casting of Orbital Prosthesis

ERNESTO H. WEISSON, MAURO FITTIPALDI, CARLOS A. CONCEPCION, DANIEL PELAEZ, LANDON GRACE, AND DAVID T. TSE

• PURPOSE: A proof-of-concept workflow study for the fabrication of custom orbital exenteration prostheses via automated noncontact scanning, 3D printing, and silicone casting.

• DESIGN: Noncomparative, interventional case series.

• METHODS: SETTING: Single-center institutional study. STUDY POPULATION: Three patients who have discontinued wearing of the ocularist-made exenteration prosthesis due to altered fit, discoloration, or material degradation. INTERVENTION PROCEDURE: A digital representation of the exenteration socket and contralateral periocular region was captured through noncontact facial topography mapping. Digital construction of the anterior prosthesis surface was based on the mirrored image of the contralateral side, and the posterior surface contour was based on orbital cavity geometry. The anterior and posterior surface details were digitally merged. A 2-piece mold was designed and produced in a 3D printer. Colorimetry was used to create a custom blend of pigments for incorporation into the Shore 40 silicone elastomer to generate a prosthesis that approximates the patient's skin tone. MAIN OUTCOME MEASURES: Prosthesis symmetry, skin tone match, comfort of wear, and appearance.

• RESULTS: The first copy of every 3D-printed orbital prosthesis using this fabrication workflow produced good symmetry, color match, and prosthesis fit. In one case, the recontoured second copy with improved prosthesis edge-to-skin interface was made without the patient present.

• CONCLUSION: A noncontact 3D scanning, computer-aided design, 3D printing, and silicone casting for fabrication of orbital prosthesis was developed and validated. This production workflow has the potential to provide an efficient, standardized, reproducible exenteration prosthesis and to overcome the principal barriers to an affordable custom prosthesis worldwide: access and cost. (Am J Ophthalmol 2020;220:27–36. © 2020 Elsevier Inc. All rights reserved.)

ORBITAL EXENTERATION IS A RADICAL SURGICAL procedure in which the eyelids, eye, and orbital contents including extraocular muscles, optic nerve, fat, and lacrimal gland are removed en bloc. This procedure is commonly performed for the treatment of malignant periocular tumors invading into the orbit, intraocular tumors with extraocular extension, or primary and secondary orbital malignancies.[1] The surgical aim is to achieve tumor-free margins. It is also performed in painful or life-threatening orbital infections or inflammations.[2] The postsurgical outcome is a bare orbital cavity.

Loss or absence of an eye and orbital contents is both physically and psychologically traumatizing and can severely affect human interactions.[3] The psychological and cosmetic rehabilitation begins shortly after socket healing with the fitting of an orbital exenteration prosthesis to approximate the form of the contralateral unaffected side. The fabrication of an exenteration prosthesis is an arduous and time-intensive process. It generally takes a certified ocularist or anaplastologist (prosthetist), who is skilled in the art, 1-2 weeks to complete the fabrication using traditional contact impression, mold-making, hand sculpting, and a variety of other technical production steps.[4] The completed static orbital prosthesis is made of a silicone elastomer consisting of fixed eyelids, an ocular prosthesis insert, and artificial eyelashes. The resulting symmetry, likeness, and color matching are heavily dependent on the experience and skill of the prosthetist. The composite unit is affixed to the entrance of the empty orbital socket with glue or double-sided tape. An ideal exenteration prosthesis should possess neutral expressiveness and closely match the nuanced skin characteristics and periocular structures of the unaffected side. A well-made orbital prosthetic device can dramatically improve a patient's self-esteem and quality of life.[5]

Making an initial or replacement orbital prosthesis can be expensive.[6,7] Generally, a silicone orbital prosthesis is expected to last 1-2 years before requiring replacement.[8,9] Prosthesis discoloration from fluid, skin oil and dirt

Accepted for publication Jun 21, 2020.

From the Nasser Ibrahim Al-Rashid Orbital Vision Research Center, Bascom Palmer Eye Institute, Department of Ophthalmology (E.H.W., C.A.C., D.P., D.T.T.), University of Miami Miller School of Medicine, Miami, Florida; Department of Mechanical and Aerospace Engineering, University of Miami (M.F.), Coral Gables, Florida; Department of Mechanical and Aerospace Engineering, North Carolina State University (L.G.,), Raleigh, North Carolina, USA.

[1] Mr Weisson and Dr Fittipaldi served jointly as first authors.

Inquiries to David T. Tse, Bascom Palmer Eye Institute, University of Miami Miller School of Medicine, 900 N.W. 17th Street, Miami, FL 33136, USA; e-mail: dtse@med.miami.edu

0002-9394/$36.00
https://doi.org/10.1016/j.ajo.2020.06.032

FIGURE 1. Instruments for noncontact facial topography mapping and 3D printing of orbital prosthesis. Left: Full Color 3D scanner. Center: Colorimeter. Right: 3D printer.

deposition, material degradation, fraying of the device edges, and altered fitting from changing soft tissue contour around the orbital entrance can affect cosmetic symmetry.[10,11] In developing countries, access to a skilled anaplastologist can be limited. As a consequence, many patients cannot afford the purchase of a prosthesis and usually cover the defect with a patch. Even after obtaining a first prosthesis, the cost of replacement is often prohibitive, such that patients resort to wearing a frayed and discolored unit, or not wearing one at all. In underdeveloped countries, particularly among children, wearing of an exenteration prosthesis is uncommon because of the rapid pace of growth and change in facial dimensions, the cost associated with each prosthesis, and the limited access to an experienced anaplastologist.

Innovation and the adoption of new technologies such as high-resolution digital scanners, computer-aided design (CAD) software for manipulation of complex three-dimensional (3D) digital data sets,[12,13] and high-resolution 3D printers can help reduce the cost and overcome the technical hurdles that limit access to facial and orbital prostheses for many patients worldwide.[14,15] The purpose of this proof-of-concept fabrication study was to illustrate a novel workflow of an orbital prosthesis fabrication using advanced digital technologies. We hypothesized that the integration of 3D facial topography capture, 3D printing, automated color matching, and CAD could reduce prosthesis cost, improve access, eliminate operator-associated variability, improve symmetry and likeness, and produce a high-quality, ready-to-wear prosthesis without prior experience in prosthesis fabrication.

PATIENTS AND METHODS

THIS IS A CASE SERIES OF 3 PATIENTS, AND NO DATA WERE analyzed to develop generalized knowledge. The authors have received a written exemption of IRB review from the University of Miami Institutional Review Board. An informed consent was obtained from each patient after full explanation of the investigative nature of the study. The study adhered to the tenets of the Declaration of Helsinki and complied with the Health Insurance Portability and Accountability Act (HIPAA). Patients included in the study were treated between January 2018 and March 2020 and had a minimum follow-up period of 6 months.

• **WORKFLOW FOR THE PRODUCTION OF A 3D-PRINTED ORBITAL PROSTHESIS:** *Facial topography capture*. The production of an orbital prosthesis begins with the scanning of the patient's facial topography using the high-resolution Artec Space Spider Hand-Held Full Color 3D scanner (Artec 3D, Luxembourg City, Luxembourg) or similar device (Figure 1). A single scan with multiple horizontal passes across the patient's face takes approximately 1 minute. Following facial topography capture, a handheld colorimeter (E-Skin by SpectroMatch Ltd, UK) is used to measure and match the skin color to a custom colorant palette in the SpectroMatch database. This process is fully automated. Measurements of certain dimensions of the patient's face, such as intercanthal distance and eyelid fissures, are taken with a caliper as redundant scaling measurements. Finally, high-definition close-up facial images are taken with a DSLR camera using a neutral gray color card for white-balance setting

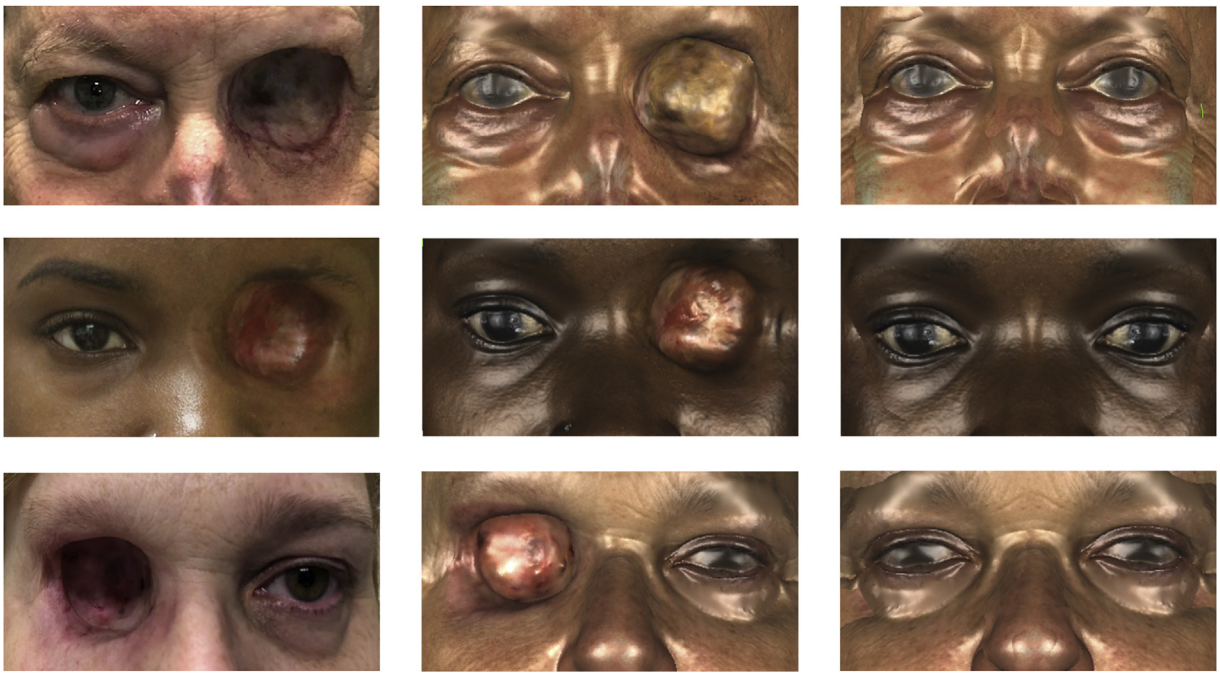

FIGURE 2. Digital scans of patient facial topography displayed on CAD software. Top Row (Case 1); Middle Row (Case 2): Bottom Row (Case 3). Left column: Pre-scan appearance of each patient. Middle Column: Corresponding digital scans of facial topography displayed on CAD software. Right Column: Computer-assisted insertion of successfully reconstructed 3D prosthesis anatomic mesh model into digital representation of patient's facial topography to ensure accurate fit.

to ensure color match reference and for comparison during detailing of the prosthesis (Figure 2, left column).

Digital adaptation of scanned facial data. Once facial topography and colorimeter recordings are completed, the raw data are preprocessed using the scanner's proprietary software, Artec Studio 12 Professional (Artec 3D, Luxembourg). All scans are then fused into a single digital mesh by performing global registration of all scanned points, removing outliers, reducing the number of polygons, and applying texture and color to the mesh. The fused mesh is exported as a Polygon File Format (.ply) into a CAD software capable of handling polygon meshes (Figure 2, middle column). The software used in this work is Geomagic Studio 12 (3D Systems, USA). A successfully reconstructed 3D prosthesis anatomic mesh model is inserted into the digital representation of patient's facial topography to ensure accurate fit (Figure 2, right column).

Digital sculpting of orbital prosthesis. Digital construction of the anterior surface of the orbital prosthesis is created by the mirrored image of the contralateral periorbital region to ensure symmetry. The posterior surface is modeled on the orbital cavity geometry to create the bulbous portion of the prosthesis that will apply gentle radial pressure in the socket for a comfortable custom fit. A plane of symmetry is approximated by selecting various points that run along the midline of the face. The plane of symmetry serves as a guide from which a duplicate of the scan is mirrored. The scan points where the original scan and the mirrored scan deviate by more than 2 mm due to the orbital defect are then determined to delineate the appropriate boundaries of the prosthesis. This is accomplished by performing a deviation analysis that finds the minimum distance between a point in the original scan and a point in the mirror scan. The colorized deviation map of the scan data is illustrated in Figure 3. The anterior and posterior surfaces are then fused together to create a watertight model of the prosthesis that conforms to the orbital cavity. To facilitate ease of insertion and to avoid uncomfortable pressure points against the constituent orbital walls, the interior of the posterior bulbous portion of the prosthesis is hollowed out to provide flexibility.

To construct the hollow posterior bulbous portion of the unit, a wax insert is designed by creating a smooth offset of the entire prosthesis by a distance of 3 mm and subtracting it from the main model. This ensures that the back of the prosthesis has a uniform thickness of 3 mm, providing it with flexibility while maintaining adequate structural rigidity. A digitized model of an ocular piece is subtracted from the anterior surface of the prosthesis to create a hollow cavity for the eyepiece to fit in the final prosthesis. Finally, ocular prosthesis orientation is verified digitally to ensure

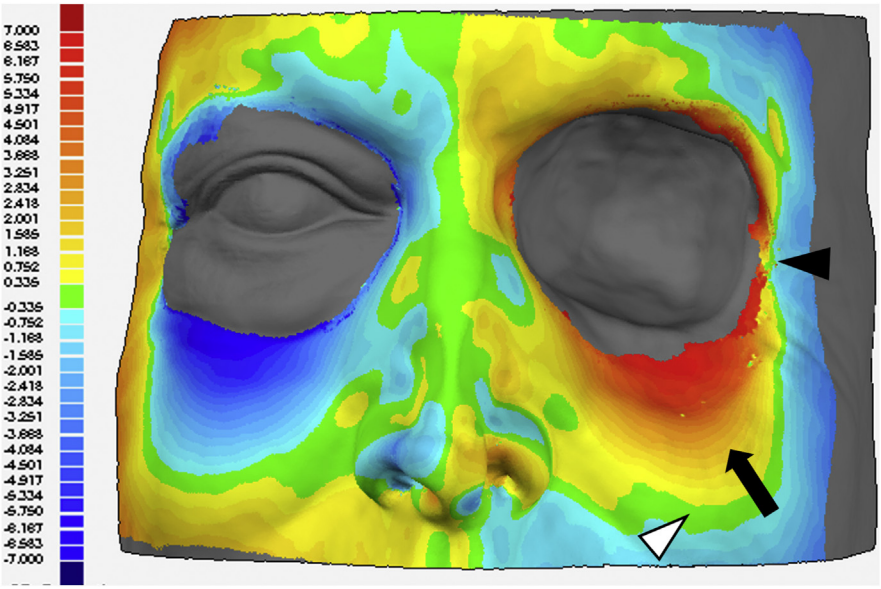

FIGURE 3. Deviation topographic map between unaffected contralateral facial contour and exenteration side of Case 1. Deviation scale (left, mm) denotes measured deviations, from blue (symmetrical), to red (maximal deviation observed). Prostheses were made to cover all periorbital areas in which the deviation score was above 2.0 mm, with pointed exceptions. Minimal deviation occurs between yellow and light blue boundary at the temporal orbital rim (black arrowhead) denoting the lateral edge of the prosthesis. The white arrowhead pointing to the green-shaded band indicates that there is minimal deviation from the contralateral side of the face. The black arrow pointing to the red shaded region indicates that there is substantial deviation; the prosthesis edge must cover all the red-shaded region and extend to the tip of the black arrow. This digitally determined edge will be integrated into the design of the mold for the final prosthesis as the edges must be carefully curved inward to effect a smooth interface with the skin.

a proper fit of the integrated ocular piece after casting as seen in Figure 4. The result of this process is a stand-alone 3D model of the prosthesis that can be positioned on the original scan of the patient to verify symmetry and gaze alignment.

Design of 3D mold. To create the mold digitally, the front and back of the prosthesis are separated along the edge and used to build a 2-piece negative mold. It is crucial that the parting line of the mold is along the prosthesis edge, which will hide the seam line caused in the fusion of both mold parts. The back mold has 2 small holes for filling of the mold: a sprue hole for injection of the polymer mixture for casting of the prosthesis, and an air hole for excess silicone and air bubbles to escape. On the diametrically opposite corners of the molds, alignment pins are created for clamping the front and back molds and to prevent sliding during silicone casting. A mold for the wax insert is designed in a similar fashion, parting the model down the center to create a 2-piece mold. The completed mold design is then exported as a binary stereolithography file (.stl) for 3D printing.

Printing of digitally designed 3D mold. Once the.stl files corresponding to the molds for the prosthesis are produced, they are printed with white acrylonitrile butadiene styrene (ABS) using an Ultimaker 3D printer (Ultimaker, Geldermalsen, Netherlands). Printing a mold generally takes approximately 20 hours to complete at a layer height resolution of 60 μm. The molds are then manually smoothed with acetone to remove any visible print lines or sharp edges (Figure 5, A).

Casting of the prosthesis. Upon printing of the final molds, silicone color samples are made according to the SpectroMatch e-Skin color codes using Electron Microscopy Sciences (EMS) Shore 40 Two-Part Clear Silicone Kit 24232-C, the same silicone used in the production of the prosthesis. Using color-corrected high-definition images taken during the scanning, a skin color is selected that best approximates the average base tone for the patient's face.

The last step before casting is the preparation of the wax insert for the hollow cavity in the posterior of the prosthesis. Using the 3D-printed positive ABS mold, a silicone negative of the wax insert is cast in the same silicone. Paraffin wax is cast into the shape of the insert using the silicone mold, as paraffin adheres to the surface of the ABS mold but not to silicone. Once the paraffin wax insert is set, it is adhered to the front face of the mold on the posterior surface of the ocular piece placeholder. The wax insert is carefully aligned using the digital design of the mold on

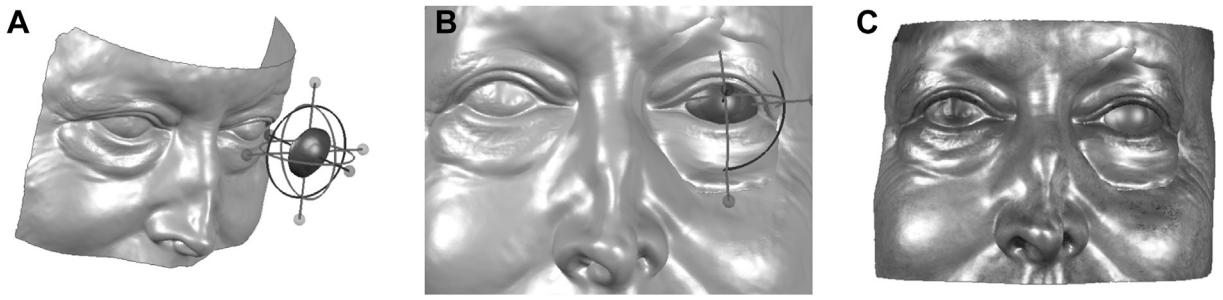

FIGURE 4. Digitally aligning the ocular piece to ensure proper gaze (Case 1). A. The ocular piece is moved into its estimated position and roughly aligned. B. Once in position, fine adjustments to gaze alignment and symmetry are made using a center-point marking on the ocular piece. C. A final review of the gaze is assessed with the ocular piece in place on reconstructed 3D prosthesis anatomic mesh model of the patient's facial topography.

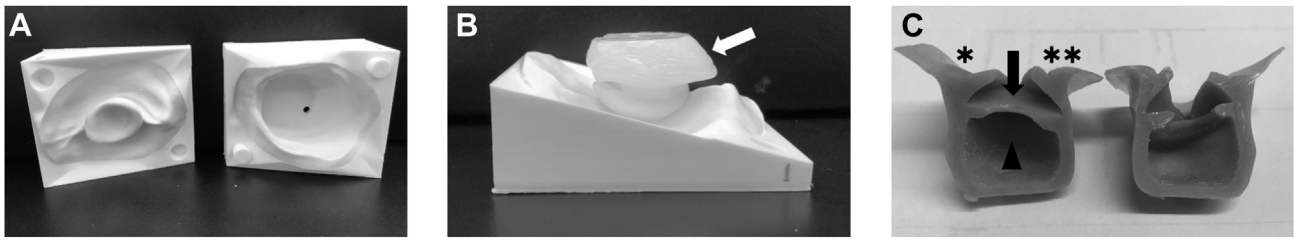

FIGURE 5. 3D-printed acrylonitrile butadiene styrene (ABS) mold and molded prosthesis (Case 1). A. The left block is the negative front mold for the anterior surface. The right block is the negative back mold for the posterior surface of the prosthesis with a sprue injection hole in the middle. B. Back mold with attached wax insert to create the hollow posterior bulb (arrow). C. Sagittal view of a bisected molded prosthesis. Top hollow space (arrow) is the pocket created to house the ocular prosthesis. Bottom hollow space (arrowhead) is the cavity of the bulbous posterior portion of the prosthesis. The upper eyelid is represented by an asterisk. The lower eyelid is represented by 2 asterisks.

Geomagic, so as to create a hollow shell of uniform thickness in the posterior surface of the prosthesis (Figure 5, B).

Finally, the silicone is prepared for casting. The total volume of material required for the prosthesis production is calculated and entered into SpectroMatch's e-Skin recipe database to obtain a recipe for the base skin tone at the required volume. The silicone is mixed with the proper ratio of SpectroMatch Quick Weigh e-Skin silicone pigments. The pigments and activator compound mixture is homogenized and degassed in a Speedmixer (FlackTek Inc, USA). The mold is clamped tight with bar clamps, applying significant pressure to ensure a proper seal, and the silicone mixture is injected through the sprue hole until excess silicone flows through the air hole and no air bubbles remain.

Proper design of the prosthesis edge is particularly important. To produce an inconspicuous interface between the prosthesis and the patient's skin, edges must be carefully tapered. The edges of the prosthesis should taper out from 0.5 to 0.3 mm, which has been determined to be sufficient for prosthesis durability while providing a satisfactory prosthesis-skin interface. A cross section of the hollow prosthesis after casting is shown in Figure 5, C.

Detailing of the silicone orbital prosthesis. The cured silicone prosthesis is removed from the mold for final detailing after a 16-hour bench cure at room temperature. The excess plastic from the rim of the prosthesis is trimmed and inspected for any deformities while casting. A layer of extrinsic coloration is applied to the surface by hand using pigments from Factor II's Extrinsic Coloration Kit KT-199 Silicone Paint Kit (Factor II Inc, USA). These pigments add details such as shading under the eye, as well as along the folds of the upper eyelid and conjunctiva to increase realism and aesthetic qualities of the prosthesis. After the silicone paint has set, the sealing and matting process takes place. In a multistep process, Factor II silicone prosthetic sealant is applied, texturized, and matted to protect the details of the prosthesis, while increasing its similarity to the tone and texture of the skin surrounding the patient's defect. Generic synthetic eyelashes are commercially available in beauty shops and pharmacies. The store-purchased synthetic eyelashes are affixed to the prostheses using clear silicone, the same type of material used for prosthesis fabrication. Using Westcott tenotomy scissors, eyelashes are trimmed to resemble the length, shape, and density of patient's contralateral side. The

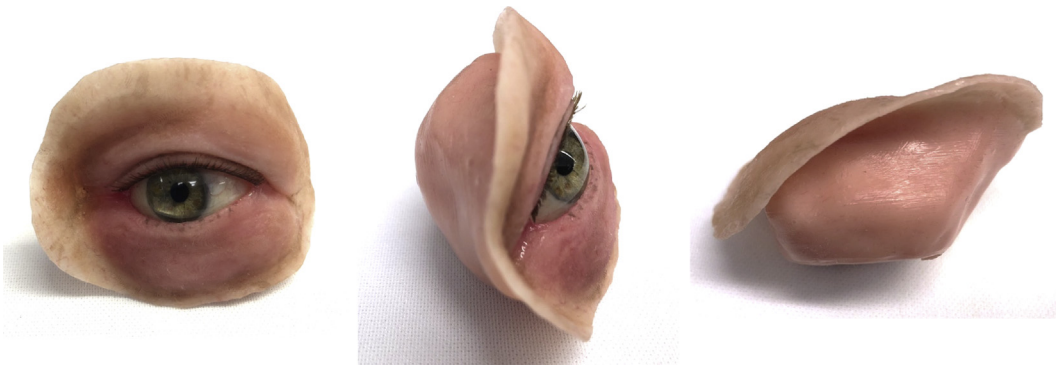

FIGURE 6. Front, sagittal, and posterior views of a completed prosthesis with extrinsic coloration applied and ocular piece inserted (case 1). This prosthesis includes an ocular piece from the patient's old unit.

important artistic judgment is to approximate the lash color, length, and contour as much as possible. No training is required for this task. A small amount of EMS clear silicone is applied to the lacus lacrimalis of the medial canthus to provide a mild sheen (Figure 6).

RESULTS

ALL PATIENTS WERE SCANNED IN CLINIC. THE APPROXIMATE total production time for a prosthesis is 46 hours. The time required in each fabrication step is summarized in the Table. This workflow with customized made-to-specification CAD design produced prostheses with excellent socket fit, symmetrical alignment to the normal side in form, and the precise pigment ratio mix yielded good color match on all patients. Two (cases 2 and 3) of the 3 orbital prostheses used the new acrylic ocular prosthesis made by a non–3D printing technique developed in our laboratory. In case 1, the ocular piece from the patient's old prosthesis was used (Figures 7 and 8). All were designed as adhesive-retained orbital prosthesis, but only 1 patient occasionally uses adhesive to secure the prosthesis. All 3 patients reported comfort of wear and described the 3D printed prosthesis with soft hollow posterior bulb as having more even distribution of pressure within the socket and better fit retention than the prostheses they had previously worn. The 3 patients in this study wear glasses with polycarbonate lens to protect the normal eye and use the frame to strategically camouflage the edges of the prosthesis.

• **CASE REPORTS:** *Case 1.* A 63-year-old man had left orbital exenteration for lacrimal gland adenoid cystic carcinoma following an institutional protocol with neoadjuvant intra-arterial chemotherapy, concurrent chemoradiation therapy, and additional cycles of adjuvant chemotherapy. He is disease-free 11 years following treatment. He had an orbital prosthesis made by the conventional method but discontinued wearing it after 2 years because of discoloration and poor fit, instead opting for a black patch. The patient's facial mapping and colorimeter readings were captured during a clinic visit in the methods described above. The completed first copy of the prosthesis was mailed to the out-of-state patient a week later. The close-up photos of the prosthesis wear were taken by the patient and e-mailed back. Based on inspection of the photographs, it was determined that the prosthesis edge at the 5-7 o'clock hour meridians were vaulted off the skin (Figure 7, A [arrow]) and the superotemporal edge was too wide and thick (Figure 7, A [arrowhead]). Using the archived digital data sets, the superotemporal edge was digitally trimmed and thickness reduced, and the inferior prosthesis edge was curved toward the skin to eliminate the vaulting. A second copy was made and mailed back to the patient. Photographs of the patient wearing the second copy showed both flaws were corrected (Figure 7, B and C). The deviation mapping guided how far the inferior edge of the prosthesis needed to curve to effect a proper interface with the skin in the second iteration.

TABLE. Approximate Manufacturing Times

Step		Time
1.	Facial topographic mapping	1 h
2.	Digital sculpting and adaptation of facial data	4 h
3.	Digital design of 3D mold	2 h
4.	Mixing pigments and silicone	1 h
5.	3D printing the digitally designed mold	20 h
6.	Casting the silicone prosthesis	16 h
7.	Detailing	2 h
Total time		46 h

Case 2. A 26-year-old woman had left orbital exenteration for fibromyxoid sarcoma at age 14 years. Her first orbital prosthesis was anchored to the frame of the

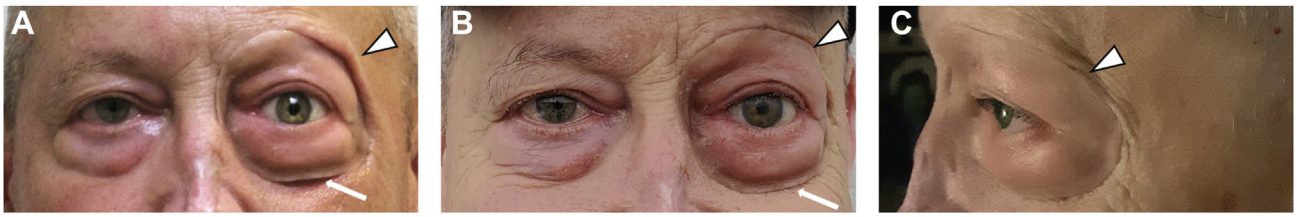

FIGURE 7. Digital modifications to generate a revision unit (Case 1). A. The first iteration of the fabricated prosthesis showed suboptimal inferior prosthesis edge–skin interface (arrow) and the superotemporal edge was too wide and thick (arrowhead). B. Using the archived digital data sets, the superotemporal edge was digitally trimmed and thickness reduced (arrowhead). The inferior edge of the prosthesis between the 5 and 7 o'clock hour meridians was thinned and tapered to eliminate the vaulting (arrow). This second iteration showed both flaws were corrected. C. Temporal view of the second iteration showing improved prosthesis-skin interface (arrowhead).

FIGURE 8. Final orbital prosthesis fitting. Top row: Case 1. Ocular prosthesis is from patient's old orbital prosthesis. Middle row: Case 2. The acrylic ocular prosthesis is made by a non–3D printing technique. Bottom row: Case 3. The acrylic ocular prosthesis is made by a non–3D printing technique.

glasses. She stopped wearing it and combs her hair over the left side of her face to cover the orbital cavity. The first iteration of her prosthesis was made without the benefit of the colorimeter for precise color determination, and the finished unit was judged to have suboptimal color tone match. The patient returned to have repeat facial scanning and a colorimeter reading using the spectrometer and the fabrication workflow described. A new prosthesis with a much better skin tone match was produced (Figure 8).

Case 3. A 53-year-old woman had right orbital exenteration for lacrimal gland adenoid cystic carcinoma following an institutional protocol with neoadjuvant intra-arterial chemotherapy, concurrent chemoradiation therapy, and additional cycles of adjuvant chemotherapy. She is disease-free 8 years following treatment. The initial prosthesis was made by an ocularist using the conventional fabrication method. She discontinued the wear of the prosthesis within a year because the fit was not optimal: her skin was sensitive to the use of

adhesives, and the unit frequently fell off the orbital rim in the presence of perspiration. The orbital prosthesis unit fabricated using facial topography mapping, 3D printing, and silicone casting method provided a more comfortable orbital fit and retention because of the bulbous posterior feature of the unit. She can now wear the prosthesis comfortably for a week without removal. The prosthesis edge–skin interface and color match were judged to be ideal by the patient (Figure 8).

DISCUSSION

INNOVATIONS IN 3D PRINTING OF CUSTOM PROSTHESES, IMplants, and devices derived from patient-specific anatomic features continue to revolutionize medicine. Applications of 3D printing of devices for medical advancement include a tracheal stent, a bionic ear, and vascular networks for perfusable engineered 3-dimensional tissues.[16–18]

In this proof-of-concept workflow study of digitally designed orbital prostheses using automated noncontact scanning, 3D printing, and silicone casting, we were successful in producing a first copy with good facial symmetry and prosthesis fit. The colorimeter provided the precise pigment ratio mix to yield good color match. The wax insert to make the bulbous posterior prosthesis surface hollow is a novel aspect of the manufacturing process to improve socket conformation and comfort of wear. Minor digital manipulation from archived data was used in one patient to refine prosthesis edge contour and skin surface interface to produce the final second copy. The recontoured second copy with improved prosthesis edge-to-skin interface was mailed back to the patient without the need for a return office visit. This validated production workflow with customized made-to-specification CAD design can provide an efficient, standardized, reproducible fabrication of an exenteration prosthesis.

In a 2019 systematic review on the computerized tools and digital techniques applied to fabricate nasal, auricular, orbital, and ocular prostheses for facial defect rehabilitation, Farook and associates[7] indicated that there is no single set of standards of fabrication exclusive to digitally designed facial prostheses. Orbital prostheses follow a similar workflow as auricular prostheses. A total of 8 reports for orbital prosthesis fabrication were identified. Data acquisition method varied, ranging from 3D photogrammetry,[14,19–21] magnetic resonance imaging, or computed tomography,[22–24] and digital camera.[25]

A review of reports relevant to this manuscript on automated noncontact techniques of orbital prosthesis fabrication showed similar yet disparate production steps when compared to our workflow. Although CAD remains the core element in transforming the automated prosthesis production process over the traditional methods of fabrication,[6,12–24,26] none of the reports describe the use of these automated technologies from digital data capture to prosthesis fabrication in a single appointment with the patient. Some projects report manually determining the symmetry plane of the patient, whereas others do not make use of the defect topography. In some cases, wax models are still produced, lengthening and complicating the fabrication process.

Four studies share some similarities to our noncontact facial topography mapping, but workflow varied.[14,15,19,20] Liu and associates[19] combined the use of a large, floor-mounted facial scanner and an intraoral scanner to acquire the digital scans. In acquiring the topography of the contralateral eye, an intraoral scanner slides over the healthy eye while protecting the eye with a light-proof contact lens. The 2 scans are merged and imported into Geomagic Studio as.stl files to digitally design the prosthesis and mold. All color matching was done by hand. Chiu and associates[20] employed 3D photogrammetry, instead of a portable scanner, with reconstruction software and a sculpting software to project the patient's mirrored eye onto the orbital defect to create the mold for 3D printing with thermoplastic polymer. Bi and associates[14] used integrated optical scanning techniques, CAD, and rapid prototyping technology to design negative molds for the fabrication of orbital prostheses. Rapid prototyping is the fast fabrication of an assembly by additive manufacturing or 3D printing. The material used was A-RTV-30 silicone, and the final prosthesis was completed by applying the extrinsic coloring to the pale-gray silicone unit, instead of an intrinsically colored unit. Yoshioka and associates[15] provided a noncontact scanning method similar to our technique, but it utilized a laser, not the less-invasive blue-light technology, to scan. The prosthesis was modeled in CAD software using the mirroring method. A 3D printer was then used to make a negative mold for a wax prototype of the prosthesis that was then fitted on the patient's face. The prototype was then packed with intrinsically colored silicone material. A high degree of artistry was required to fit and texturize the wax model prior to making the definitive copy with silicone. Coloring was done by hand, as there was no description of an automated method of standardizing the base skin color with an objective, reproducible recipe.

Our findings also demonstrated that our novel process does not require access to a skilled prosthetist, and thus has the potential to provide an efficient, standardized fabrication process for custom orbital prosthesis regardless of a patient's physical location. The archived data sets allow for quick, precise digital sculpting to refine the prosthesis edge–skin interface or correction of any flaws with the fabricated unit without the patient being physically present. Furthermore, cost and fabrication time of subsequent prostheses in the event of loss, damage, or change in cosmetic match is dramatically reduced by retaining the digital and physical versions of the prosthesis and molds. A replacement unit would not require the patient to be

present unless replacement was necessitated by a major change in facial topography. It is important to note that none of the authors had training in prosthesis fabrication or consulted an ocularist at any time, demonstrating the ability of this process to improve global access to orbital prostheses.

Because of the versatility of remote file-sharing technologies, we envision a patient's facial topography and skin color tone can be captured on-site, out-of-state, or in remote parts of the world and uploaded to a central location for digital modeling and fabrication. The only equipment needed at the scanning site are a high-resolution scanner, a colorimeter, and a high-resolution camera. Once the digital scanning data are captured and archived, manufacturing a replacement prosthesis can be centralized without the need for another scanning session. Traditional methods of facial prostheses fabrication rely on molds made of dental stone that degrade with every consecutive cast, limiting their reusability.[27] The 3D-printed ABS molds used in this workflow have the rigidity and chemical compatibility and stability required to withstand several iterations of silicone casting.[26,28] Furthermore, new molds can be generated from the digitized data at will, eliminating the need for the patient to return for another scanning. An additional benefit of this workflow is the adaptability in integrating new materials as they become available: the Ultimaker 3D printer used in this study can handle a variety of thermoplastic filaments to produce molds of varying chemical and mechanical properties, and the use of silicone can be replaced with any room temperature–curing thermosetting elastomer.

The rate-limiting steps of this fabrication workflow are the 3D printing of the digitally designed mold and casting of the silicone prosthesis, with approximate durations of 20 and 16 hours, respectively (Table). However, it should be noted that this proof-of-principle study was carried out using a benchtop hobby 3D printer. As newer technologies in 3D printers become available, or with the use of industrial-type production 3D printers, we anticipate that printing time of the ABS mold can be shortened dramatically. Similarly, with the emergence of innovative print materials capable of directly printing ultra-realistic anatomic structures in full color may supplant the need for mold production altogether. The experience gained in digital sculpting and adaptation of facial data to design the prosthesis, particularly the edge–skin interface, remains a key step in fabricating a near-perfect first copy.

In summary, our proof-of-concept study demonstrates the ease of use and integration of advanced digital technologies for the efficient production of a complex orbital prosthesis that traditionally requires a trained anaplastologist skilled in the art and knowledge of mold making to hand-sculpt the unit. Our findings show that the described production workflow can produce an orbital prosthesis with good facial symmetry, skin tone match, prosthesis fit and comfort of wear. The archived data sets allow for quick, precise digital manipulation to refine the prosthesis edge–skin interface or touch-up of any flaws in the fabricated unit without the patient being present. This novel facial topography mapping, 3D printing, and silicone casting fabrication method has the potential to improve global access to orbital prostheses for an underserved population.

FUNDING/SUPPORT: THIS WORK WAS SUPPORTED IN PART BY NIH CENTER CORE GRANT P30EY014801; RESEARCH TO PREVENT Blindness Unrestricted Grant, Inc, New York, New York; and the Dr Nasser Ibrahim Al-Rashid Orbital Vision Research Fund. The sponsor or funding organization had no role in the design or conduct of this research. Financial Disclosures: The authors indicate no financial support or conflicts of interest. All authors attest that they meet the current ICMJE criteria for authorship.

REFERENCES

1. Nassab RS, Thomas SS, Murray D. Orbital exenteration for advanced periorbital skin cancers: 20 years experience. *J Plast Reconstr Aesthet Surg* 2007;60(10):1103–1109.
2. Kennedy RE. Indications and surgical techniques for orbital exenteration. *Adv Ophthalmic Plast Reconstr Surg* 1992;9:163–173.
3. Markt JC, Lemon JC. Extraoral maxillofacial prosthetic rehabilitation at the M. D. Anderson Cancer Center: a survey of patient attitudes and opinions. *J Prosthet Dent* 2001;85(6):608–613.
4. Shrestha B, Goveas R, Thaworanunta S. Rapid fabrication of silicone orbital prosthesis using conventional methods. *Singapore Dent J* 2014;35:83–86.
5. Wang J, Zhang H, Chen W, Li G. The psychosocial benefits of secondary hydroxyapatite orbital implant insertion and prosthesis wearing for patients with anophthalmia. *Ophthal Plast Reconstr Surg* 2012;28(5):324–327.
6. He Y, Xue GH, Fu JZ. Fabrication of low cost soft tissue prostheses with the desktop 3D printer. *Sci Rep* 2014;4:6973.
7. Farook TH, Jamayet NB, Abdullah JY, Rajion ZA, Alam MK. A systematic review of the computerized tools and digital techniques applied to fabricate nasal, auricular, orbital and ocular prostheses for facial defect rehabilitation. *J Stomatol Oral Maxillofac Surg* 2020;121(3):268–277.
8. Shrestha B, Thaworanunta S. Orbital prosthesis fabrication: current challenges and future aspects. *Open Access Surg* 2016;2016(1):21–28.
9. Karakoca S, Aydin C, Yilmaz H, Bal BT. Retrospective study of treatment outcomes with implant-retained extraoral prostheses: survival rates and prosthetic complications. *J Prosthet Dent* 2010;103(2):118–126.
10. Aggarwal H, Kumar P, Singh SV. Modified technique to improve fabrication and outcome of definitive orbital prosthesis. *Orbit* 2016;35(2):66–68.

11. Pruthi G, Jain V, Rajendiran S, Jha R. Prosthetic rehabilitation after orbital exenteration: a case series. *Indian J Ophthalmol* 2014;62(5):629–632.
12. Sun J. Imperfect symmetry transform for orbital prosthesis modelling. *Rapid Prototyping J* 2013;19(3):180–188.
13. Li S, Xiao C, Duan L, Fang C, Huang Y, Wang L. CT image-based computer-aided system for orbital prosthesis rehabilitation. *Med Biol Eng Comput* 2015;53(10):943–950.
14. Bi Y, Wu S, Zhao Y, Bai S. A new method for fabricating orbital prosthesis with a CAD/CAM negative mold. *J Prosthet Dent* 2013;110(5):424–428.
15. Yoshioka F, Ozawa S, Okazaki S, Tanaka Y. Fabrication of an orbital prosthesis using a noncontact three-dimensional digitizer and rapid-prototyping system. *J Prosthodont* 2010;19(8):598–600.
16. Mannoor MS, Jiang Z, James T, et al. 3D printed bionic ears. *Nano Lett* 2013;13(6):2634–2639.
17. Zopf DA, Hollister SJ, Nelson ME, Ohye RG, Green GE. Bioresorbable airway splint created with a three-dimensional printer. *N Engl J Med* 2013;368(21):2043–2045.
18. Miller JS, Stevens KR, Yang MT, et al. Rapid casting of patterned vascular networks for perfusable engineered three-dimensional tissues. *Nat Mater* 2012;11(9):768–774.
19. Liu H, Bai S, Yu X, Zhao Y. Combined use of a facial scanner and an intraoral scanner to acquire a digital scan for the fabrication of an orbital prosthesis. *J Prosthet Dent* 2019;121(3):531–534.
20. Chiu M, Hong SC, Wilson G. Digital fabrication of orbital prosthesis mold using 3D photography and computer-aided design. *Graefes Arch Clin Exp Ophthalmol* 2017;255(2):425–426.
21. Reitemeier B, Notni G, Heinze M, Schone C, Schmidt A, Fichtner D. Optical modeling of extraoral defects. *J Prosthet Dent* 2004;91(1):80–84.
22. Ciocca L, Scotti R. Oculo-facial rehabilitation after facial cancer removal: updated CAD/CAM procedures: a pilot study. *Prosthet Orthot Int* 2014;38(6):505–509.
23. Alam MS, Sugavaneswaran M, Arumaikkannu G, Mukherjee B. An innovative method of ocular prosthesis fabrication by bio-CAD and rapid 3-D printing technology: a pilot study. *Orbit* 2017;36(4):223–227.
24. Ruiters S, Sun Y, de Jong S, Politis C, Mombaerts I. Computer-aided design and three-dimensional printing in the manufacturing of an ocular prosthesis. *Br J Ophthalmol* 2016;100(7):879–881.
25. Buzayan MM, Ariffin YT, Yunus N, Mahmood WA. Ocular defect rehabilitation using photography and digital imaging: a clinical report. *J Prosthodont* 2015;24(6):506–510.
26. Qiu J, Gu XY, Xiong YY, Zhang FQ. Nasal prosthesis rehabilitation using CAD-CAM technology after total rhinectomy: a pilot study. *Support Care Cancer* 2011;19(7):1055–1059.
27. Karakoca-Nemli S, Aydin C, Yilmaz H, Bal BT. A method for fabricating an implant-retained orbital prosthesis using the existing prosthesis. *J Prosthodont* 2011;20(7):583–586.
28. Ng CT, Susmel L. Notch static strength of additively manufactured acrylonitrile butadiene styrene (ABS). *Add Manuf* 2020;34:101212.